Difunctionalised Chemosensors Containing Electroactive and Fluorescent Signalling Subunits

Félix Sancenon,[a] Angel Benito,[a] Francisco J. Hernández,[a] José M. Lloris,[a] Ramón Martínez-Máñez,*[a] Teresa Pardo,[a] and Juan Soto[a]

Keywords: Ferrocene / Anthracene / Fluorescence / Chemosensors

The new ligands 13-anthrylmethyl-7-ferrocenylmethyl-1,4,10-trioxa-7,13-diaza-cyclopentadecane (L^1) and 1-anthrylmethyl-4,8,11-ferrocenylmethyl-1,4,8,11-tetraaza-cyclotetradecane (L^2) have been synthesised, characterised, and their potential activity as chemosensors towards the metal cations Ni^{2+}, Cu^{2+}, Zn^{2+}, Cd^{2+}, Hg^{2+} and Pb^{2+} studied in 1,4-dioxane/water (70:30, v/v). Both ligands L^1 and L^2 are difunctionalised receptors containing redox-active (ferrocene) and fluorescent (anthracene) signalling subunits. The crystal structures of $[H_2L^1][PF_6]_2$ and $[CuL^2][PF_6]_2$ were determined by single-crystal X-ray procedures. Potentiometric experiments in dioxane/water (70:30, v/v; 0.1 M KNO_3; 25.0 ± 0.1 °C) for L^1 and L^2 allowed the determination of protonation constants and complex stability constants with the Cu^{2+} and Pb^{2+} metal ions. They form stable complexes with both ligands and show stability constants with values close to those reported for similar complexes. The electrochemical and fluorescence behaviour of L^1 and L^2 was studied as a function of the pH and in the presence of the Ni^{2+}, Cu^{2+}, Zn^{2+}, Cd^{2+}, Hg^{2+}, and Pb^{2+} metal cations. The fluorescence and electrochemical response of L^1 and L^2 is pH-dependent. Ligand L^1 was able to electrochemically and selectively sense Pb^{2+} whereas L^2 sensed Cu^{2+}, Zn^{2+}, and Cd^{2+} using electrochemical techniques. The maximum electrochemical shift (ca. 57 mV) was found for L^2 in the presence of Cu^{2+} at pH = 8. Fluorescence studies showed that the emission intensities of L^1 and L^2 were selectively enhanced in the presence of Cu^{2+}. Additionally, the $[Cu(L^2)]^{2+}$complex acted as anion-sensing receptor in acetonitrile. The oxidation potential of the ferrocenyl group of the $[Cu(L^2)]^{2+}$complex was cathodically shifted upon addition of anions. The largest electrochemical shift was observed in the presence of fluoride (210 mV). The fluorescence emission of the anthracene groups in $[Cu(L^2)]^{2+}$ was enhanced in the presence of fluoride, nitrate, and dihydrogenophosphate.

Introduction

The design of functionalised receptors for the development of potential chemosensors is a field of active research. Of especial interest is the synthesis of molecules capable of amplifying microscopic events (for instance the presence of a target guest in a certain solution) to macroscopic levels.[1] This sensing function is generally achieved by the coupling of two well-defined parts, (i) selective binding sites and (ii) signalling subunits. This second component can be classified by the type of signal output; colour changes,[2] redox shifts,[3] and fluorescence quenching or enhancement[4] are among some commonly observed signals. Sensing molecules showing those changes can be built by attaching chromogenic units,[5] redox-active groups,[6] or fluorescent signalling subunits,[7] respectively, near the binding sites. Whereas the ligand−guest interaction is controlled by well-known binding rules (this is particularly true for ligand−cation interactions) the communication with the signalling subunit is more subtle. In some cases this is even unpredictable due to the competition of several processes, namely changes in photoelectron transfer or energy transfer paths, changes in redox properties of the receptor, etc. These new molecules are important because they will surely be the chemical active part of new sensing devices. For instance, receptors able to change spectroscopic properties (colour or fluorescence) in the presence of target substrates are of application in optical fibre devices,[8] whereas changes in redox potential upon addition of certain guests could be of application in the development of amperometric sensing devices.[9]

Despite the development of these individual areas, there are very few examples of molecules containing more than one type of signalling unit.[10] These systems can be important in the development of a new family of ion chemosensors that can either be able to sense different guests or display two or more macroscopic observable events upon addition of a certain analyte. Towards this goal, we have synthesised macrocyclic polyaza or oxaaza components and have functionalised them with both ferrocenyl and anthryl groups. Ferrocene is a well-known electro-active signalling subunit. Anthracene can act as either an electro- or photo-active

[a] Departamento de Química, Universidad Politécnica de Valencia,
Camino de Vera s/n, 46071 Valencia, España
Fax: (internat.) + 34-96/387-7349
E-mail: rmaez@qim.upv.es
Supporting information for this article is available on the WWW under http://www.eurjic.com or from the author.

  1434−1948/02/0404−0866 $ 17.50+.50/0 *Eur. J. Inorg. Chem.* **2002**, 866−875

group. Moreover, we have used the anthracene group because of its photophysical properties, and therefore we will refer to it as a fluorescent signalling subunit.

Results and Discussion

The new ligands L^1 and L^2 (Scheme 1) were synthesised according to a two-step reaction. Thus, reaction of 9-(chloromethyl)anthracene and the corresponding macrocycle (1:1 molar ratio) allowed isolation of the anthrylmethyl-functionalised derivatives that were further treated with an excess of (ferrocenylmethyl)trimethylammonium iodide in acetonitrile to give L^1 and L^2 in rather good yield. ^1H and ^{13}C NMR and mass spectra of L^1 and L^2 were consistent with the proposed formulation. Additionally, the crystal structures of the protonated form of L^1 and the Cu^{2+} complex of L^2 were determined using single-crystal X-ray procedures (see below).

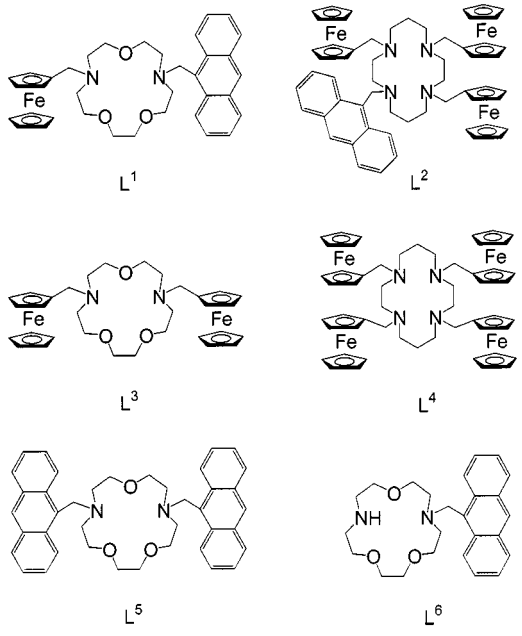

Scheme 1

L^1 and L^2 are rare examples of molecules containing redox-active and fluorescence signalling subunits. The following work has been devoted to characterise the ligands, their solution behaviour and their electrochemical and emission properties in the presence of transition metal ions and anions.

Crystal Structure of $[H_2L^1][PF_6]_2$

Addition of aqueous $[NH_4][PF_6]$ to acetonitrile solutions of L^1 allowed us to isolate the $[H_2L^1][PF_6]_2$ salt as a yellow solid. Suitable crystals of this compound for single-crystal X-ray diffraction techniques were obtained by slow diffusion of ether into dichloromethane solutions of $[H_2L^1][PF_6]_2$. The molecular structure consists of $[H_2L^1]^{2+}$ cations and PF_6^- anions linked ionically. The anthryl and cyclopentadienyl groups are planar within the experimental error and the ferrocenyl moiety adopts a nearly eclipsed conformation. The Fc−Cp(centroid) distances are 1.631 and 1.639 Å. A view of the $[H_2L^1]^{2+}$ cation and selected bond lengths and angles have been included as Supporting Information (see footnote on the first page of this article).

Crystal Structure of $[CuL^2][PF_6]_2 \cdot CH_2Cl_2$

The $[CuL^2][PF_6]_2$ complex was obtained by reaction of L^2 with copper(II) nitrate in acetonitrile and further addition of aqueous $[NH_4][PF_6]$. Suitable crystals for X-ray diffraction were obtained by diffusion of ether into dichloromethane solutions of the complex. Table 1 gives selected bond lengths and angles. Figure 1 shows a view of the compound. The molecular structure consists of cationic $[CuL^2]^{2+}$ and PF_6^- anions as counterions. Molecules of dichloromethane complete the packing. The Cu^{2+} atom is coordinated by the four nitrogen atoms of the macrocycle, giving a distorted square-planar geometry. Three nitrogen atoms are also covalently bonded to three ferrocenylmethyl centres, whereas one nitrogen atom is attached to an anthrylmethyl group. The Cu−N distances range from 2.116(7) to 2.152(7), averaging 2.127 Å. Some bond angles around Cu^{2+} are far from the ideal square-planar geometry, for instance N(3)−Cu(1)−N(2), N(3)−Cu(1)−N(1), and N(4)−Cu(1)−N(1) are 86.8(3), 151.2(3), and 85.7(3), respectively. The four nitrogen atoms define a plane within ±

Table 1. Selected distances and angles for compound $[CuL^2][PF_6]_2$

Distances [Å]			
Cu(1)−N(1)	2.152(7)	Cu(1)−N(2)	2.123(7)
Cu(1)−N(3)	2.116(7)	Cu(1)−N(4)	2.116(7)
N(1)−C(10)	1.465(11)	N(1)−C(1)	1.511(10)
N(1)−C(44)	1.510(11)	N(2)−C(3)	1.492(11)
N(2)−C(4)	1.498(12)	N(2)−C(11)	1.499(11)
N(3)−C(6)	1.454(11)	N(3)−C(5)	1.47(11)
N(3)−C(22)	1.532(11)	N(4)−C(9)	1.472(12)
N(4)−C(8)	1.483(11)	N(4)−C(33)	1.534(8)
Angles (°)			
N(3)−Cu(1)−N(4)	93.4(3)	N(3)−Cu(1)−N(2)	86.8(3)
N(4)−Cu(1)−N(2)	176.0(3	N(3)−Cu(1)−N(1)	151.2(3)
N(4)−Cu(1)−N(1)	85.7(3)	N(2)−Cu(1)−N(1)	92.2(3)
C(10)−N(1)−C(44)	112.7(6)	C(10)−N(1)−C(1)	107.2(7)
C(44)−N(1)−C(1)	112.6(7)	C(10)−N(1)−Cu(1)	101.5(5)
C(44)−N(1)−Cu(1)	111.7(5)	C(1)−N(1)−Cu(1)	110.5(5)
C(3)−N(2)−C(4)	107.7(6)	C(3)−N(2)−C(11)	112.4(7)
C(4)−N(2)−C(11)	107.1(7)	C(3)−N(2)−Cu(1)	110.4(5)
C(4)−N(2)−Cu(1)	103.6(5)	C(11)−N(1)−Cu(1)	114.9(5)
C(6)−N(3)−C(5)	109.0(6)	C(6)−N(3)−C(22)	111.3(7)
C(5)−N(3)−C(22)	109.1(7)	C(6)−N(3)−Cu(1)	113.6(6)
C(5)−N(3)−Cu(1)	103.9(6)	C(22)−N(3)−Cu(1)	109.5(5)
C(9)−N(4)−C(8)	108.7(7)	C(9)−N(4)−C(33)	107.7(6)
C(8)−N(4)−C(33)	110.6(6)	C(9)−N(4)−Cu(1)	104.6(5)
C(8)−N(4)−Cu(1)	111.3(5)	C(33)−N(4)−Cu(1)	113.5(4)
C(2)−C(1)−N(1)	117.1(8)	C(1)−C(2)−C(3)	114.6(8)
N(2)−C(3)−C(2)	114.9(7)	N(2)−C(4)−C(5)	110.6(7)
N(3)−C(5)−C(4)	111.3(7)	N(3)−C(6)−C(7)	116.4(7)
C(6)−C(7)−C(8)	114.6(8)	N(4)−C(8)−C(7)	115.2(7)
N(4)−C(9)−C(10)	110.8(7)	N(1)−C(10)−C(9)	112.4(7)

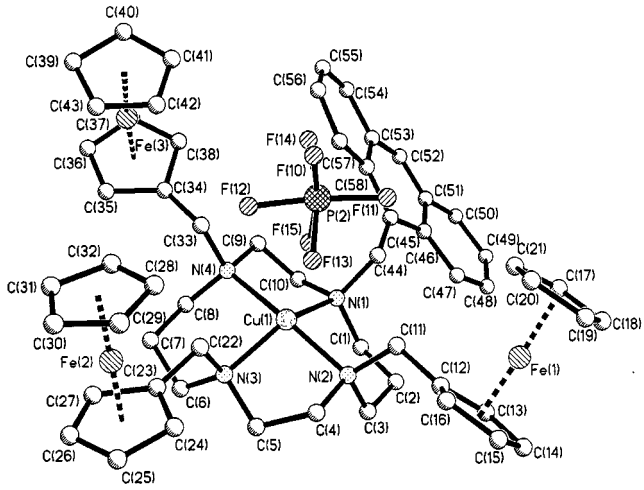

Figure 1. Molecular structure of the $[CuL^2]^{2+}$ cation

0.23 Å and the copper atom is out-of-plane by ± 0.30 Å. The deviation from the ideal geometry is mainly induced by the cyclam unit that adopts a configuration with the four nitrogen atoms pointing above the N4 plane. This has been reported to be the thermodynamically less favourable isomer.[11] However, the conformation of tetrafunctionalised cyclam derivatives containing the four groups above the N4 plane is not unusual and has also been found in complexes such as $[Ni(Me_4cyclam)]^{2+}$, Me_4cyclam = 1,4,8,11-tetramethyl-1,4,8,11-tetraazacyclotetradecane, and in the nickel(II) complex of L^4.

It is remarkable that the molecular assembly of Cu^{2+} and the ligand L^2 leads to the formation of a host molecule containing a cavity built with three ferrocenylmethyl groups and one anthrylmethyl group. In the crystal structure this cavity is filled by one PF_6^- counterion. In fact, there is a very close contact between the Cu^{2+} and the F(15) atom [Cu^{2+}···F(15) 2.47 Å]. Figure 2 also shows as an alternative view, with the space-filling representation emphasising the electro-photo-active cavity and the host−guest association.[12] No significant distortions were found in the ferrocenylmethyl and anthrylmethyl groups. The ferrocenyl units adopt the usual sandwich conformation with the cyclopentadienyl rings parallel within the experimental error. Fe-Cp(centroid) distances range from 1.621 to 1.659, averaging 1.637 Å.

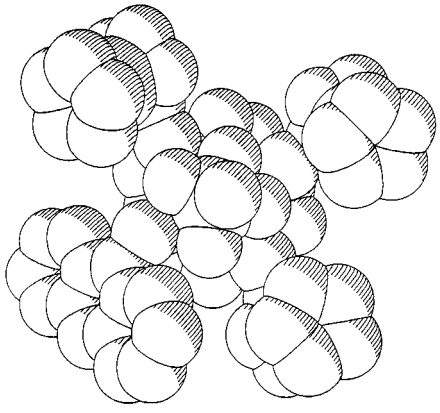

Figure 2. the space-filling representationof the $[CuL^2]^{2+}$ cation

Potentiometric Studies

Protonation constants determined potentiometrically in 1,4-dioxane/water (70:30 v/v; 25 °C; 0.1 M potassium nitrate) are shown in Table 2. As expected, L^1 and L^2 show two and four protonation processes, respectively. Ligand L^1 displays stepwise protonation constants close to those reported[13] for L^3. Ligand L^4 is a cyclam derivative, and it shows the two first protonations being much more basic than the last two. A similar behaviour was found for cyclam itself and other cyclam derivatives.[14] Figure 3 shows the distribution diagram of the L^1/H^+ and L^2/H^+ systems.

Table 2. Stepwise protonation constants for L^1 and L^2 in dioxane/water (70:30 v/v; 25 °C; 0.1 M potassium nitrate)

Reaction	L^1	L^2
$L + H^+ = [HL]^+$	8.14(2)	8.91(2)
$[HL]^+ + H^+ = [H_2L]^{2+}$	5.80(2)	6.56(1)
$[H_2L]^{2+} + H^+ = [H_3L]^{3+}$		2.71(3)
$[H_3L]^{3+} + H^+ = [H_4L]^{4+}$		2.36(1)

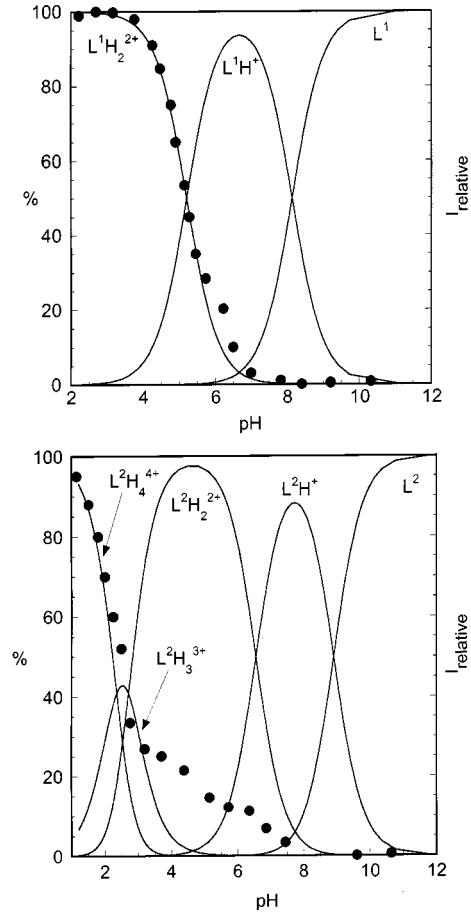

Figure 3. Distribution diagrams of the species for a) L^1/H^+ and b) L^2/H^+ (full line) and the fluorescence emission titration curves (•) for those systems

Stability constants for the formation of complexes of L^1 and L^2 with Cu^{2+}, Pb^{2+} in dioxane/water (70:30, v/v) mixtures are shown in Table 3. Both metal ions form with the receptors here considered stable $[ML]^{2+}$ complexes. Figures 4 and 5 show the distribution diagram of the $L/Cu^{2+}/H^+$ and $L/Pb^{2+}/H^+$ systems (L = L^1 or L^2). In general, the formation stability constants obtained are in line with those reported for related complexes.[14] Receptor L^2 is a tetraaza macrocycle, and displays larger stability constants with Cu^{2+} than with Pb^{2+}. In fact, the stability constant of the $L^2 + M^{2+} = [M(L^2)]^{2+}$ process is 10^3 times larger for Cu^{2+} than for Pb^{2+}. In contrast, when the N-donor atoms are partially replaced with O-donor atoms the affinity for Cu^{2+} is considerably reduced and the stability constants for the formation of the $[M(L^1)]^{2+}$ complexes are similar for Cu^{2+} and Pb^{2+} (log$K$ = 5.23 for copper and log$K$ = 5.12 for lead). These stability constants are not very different to those found for L^3 with the same metal ions {log$K$ = 6.27 and log$K$ = 6.43, for the formation of the $[M(L^3)]^{2+}$ complexes with Cu^{2+} and Pb^{2+}, respectively}.[13]

Table 3. Stability constants (log K) for the formation of Cu^{2+} and Pb^{2+} complexes of L^1 and L^2 in dioxane/water (70:30, v/v; 25 °C; 0.1 M potassium nitrate)

Reaction	L^1	L^2
$Cu^{2+} + L + H^+ = [Cu(HL)]^{3+}$	12.85(4)	14.05(4)
$Cu^{2+} + L = [Cu(L)]^{2+}$	5.23(2)	9.67(1)
$Cu^{2+} + L + H_2O = [Cu(L)(OH)]^+ + H^+$	−1.84(2)	0.56(4)
$Cu^{2+} + L + 2H_2O = [Cu(L)(OH)_2] + 2H^+$	−13.13(3)	−9.34(3)
$Pb^{2+} + L + H^+ = [Pb(HL)]^{3+}$	11.15(3)	13.45(4)
$Pb^{2+} + L = [Pb(L)]^{2+}$	5.12(1)	6.31(3)
$Pb^{2+} + L + H_2O = [Pb(L)(OH)]^+ + H^+$	−2.72(1)	−0.70(3)
$Pb^{2+} + L + 2H_2O = [Pb(L)(OH)_2] + 2H^+$	−12.81(3)	−10.12(4)

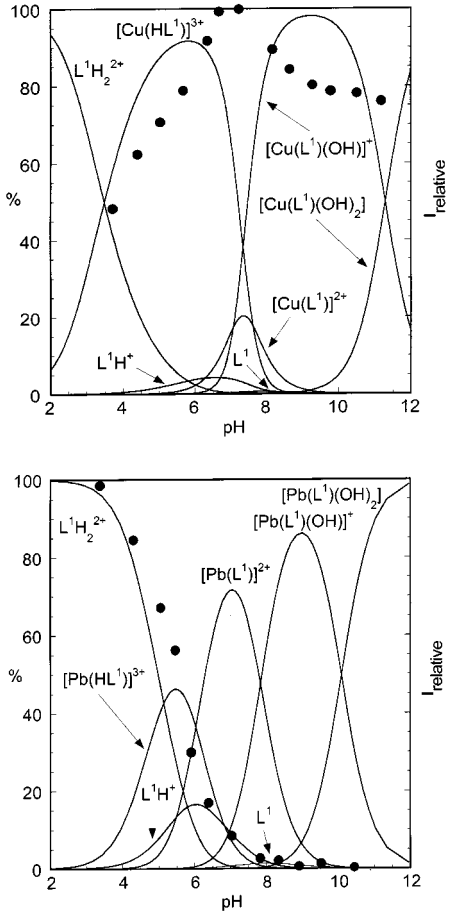

Figure 4. Distribution diagrams of the species for a) $L^1/Cu^{2+}/H^+$ and b) $L^1/Pb^{2+}/H^+$ (full line) and the fluorescence emission titration curves (•) for those systems

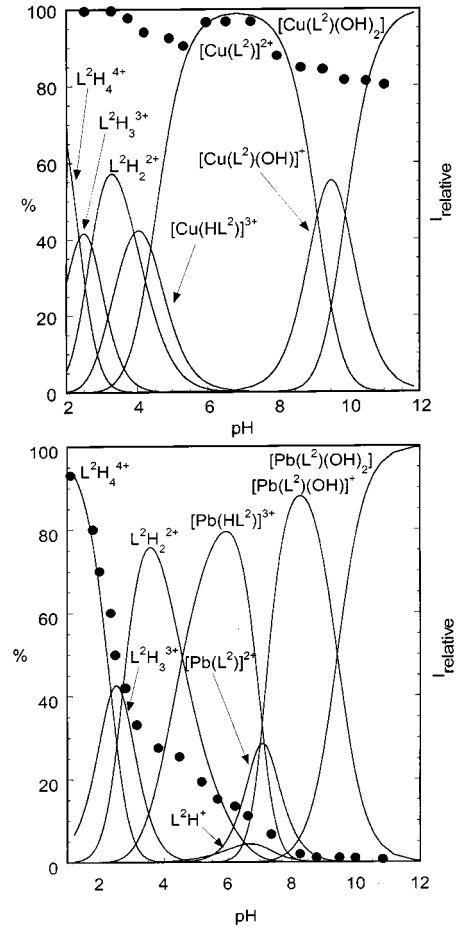

Figure 5. Distribution diagrams of the species for a) $L^2/Cu^{2+}/H^+$ and b) $L^2/Pb^{2+}/H^+$(full line) and the fluorescence emission titration curves (•) for those systems

Cation Sensing

Electrochemical Behaviour

The redox potentials of both L^1 and L^2 are pH-dependent. When basic solutions of L^1 and L^2 are acidified a steady displacement of $E_{1/2}$ ($E_{1/2}$ = half-wave potential) to more anodic potentials was observed. This is a known behaviour, attributed to the protonation of the amino groups and therefore to the formation of positively charged species that are more difficult to be oxidised.[15] The difference found between the oxidation potential under basic (pH ≈ 12) and acidic (pH ≈ 2) conditions was 140 and 110 mV for L^1 and L^2, respectively. We have also electrochemically

studied the variation of $E_{1/2}$ versus pH for the $L/H^+/M^{2+}$ systems (L = L^1 or L^2; M = Ni^{2+}, Cu^{2+}, Zn^{2+}, Cd^{2+}, Hg^{2+} or Pb^{2+}; M^{2+}/L molar ratio = 1). In order to rationalise those data the difference between $E_{1/2}$ for the receptor/metal system and that for the free receptor [$\Delta E_{1/2}$ = $E_{1/2}$(receptor/metal) − $E_{1/2}$(receptor)] was monitored at different pH values from 2 to 12. Figure 6 (top) shows $\Delta E_{1/2}$ versus pH for L^1 in the presence of Pb^{2+}. For other metal ions (Ni^{2+}, Cu^{2+}, Zn^{2+}, Cd^{2+}, and Hg^{2+}) $\Delta E_{1/2}$ is less than 5 mV (not shown). Ligand L^1 was able to electrochemically recognise Pb^{2+} over other common, typically present (in water samples) metal ions in the pH range of 5 to 7.5, although the maximum shift found of 25 mV at pH = 6.5 is rather small. Figure 6 (bottom) displays the electrochemical response found for L^2 as a function of the pH in the presence of Cu^{2+}, Zn^{2+}, and Cd^{2+}. No electrochemical shift was induced for Ni^{2+}, Hg^{2+}, and Pb^{2+}. The Cu^{2+}, Cd^{2+}, and Zn^{2+} ions change the oxidation potential of the L^2 ligand in a wide pH range, the maximum shift being observed for Cu^{2+} at pH = 8 (ca. 57 mV).

Comparison between the electrochemical response in Figure 6 and the distribution diagrams in Figures 4 and 5 allows a determination of the species responsible for the electrochemical shift. Thus, the $[Pb(L^1)]^{2+}$ complex exists in the pH range 6−8, at which the redox potential of the ferrocenyl groups suffer an anodic shift of ca. 25 mV with respect to that of the L^1 ligand. Comparison between Figure 5 (top) and Figure 6 (bottom) also suggests that it is the existence in solution of the $[Cu(L^2)]^{2+}$ complex that induces anodic shifts of up to 60 mV. It seems that there is a correlation between the presence, in solution, of the $[M(L)]^{2+}$ species and the electrochemical response. In this sense the absence of an electrochemical signal for the L^1/Cu^{2+} and L^2/Pb^{2+} systems might be related to the appearance of the $[Cu(L^1)]^{2+}$ and $[Pb(L^2)]^{2+}$ complexes as minor species [see Figure 4 (top) and Figure 5 (bottom)].

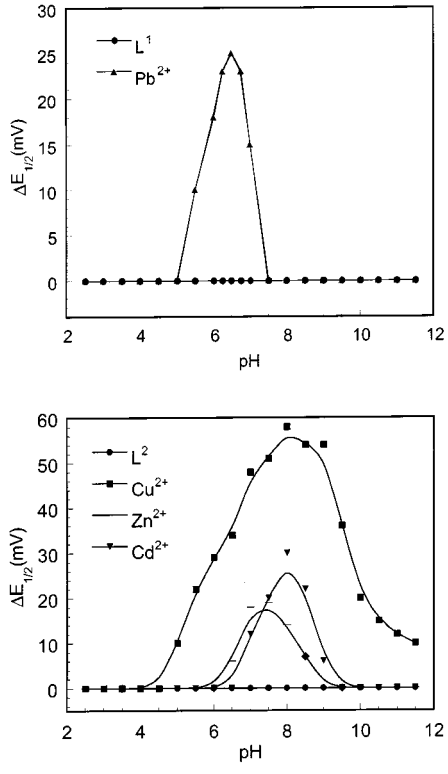

Figure 6. Oxidation potential shift ΔE [defined as $E_{1/2}$(receptor + metal ion) − $E_{1/2}$(receptor)] of a) L^1 and b) L^2 as a function of the pH in the presence of certain metal ions

At this point, it might be interesting to compare the electrochemical response of L^1 and L^2 with that previously reported for the L^3 and L^4 ferrocene-functionalised ligands. L^3 displays a large electrochemical recognition for Pb^{2+} (ca. −60 mV), although other heavy metal ions such as Cd^{2+} and Hg^{2+} also produce significant shifts (ca. −35 mV).[13] Additionally, the electrochemical shift in the presence of Pb^{2+} for L^1 is anodic but was reported to be cathodic for L^3. We have recently pointed out that in these systems, where there is no electronic communication through the bond between the metal centre and the signalling subunits, the electrochemical shift is mainly controlled by the nature of the complex formed at a certain pH and the distance between the positively charged metal centre and the ferrocenyl unit. The significant difference between the electrochemical response of L^1 and L^3 shows how subtle differences in the receptor (one or two ferrocenyl units) have significant influence in the electrochemical response. The receptor L^4 is able to electrochemically detect Cu^{2+}, Zn^{2+}, and Cd^{2+} in a wide pH range over Ni^{2+} and Pb^{2+}. This is a similar response to that observed for L^2. However, the maximum shift for L^2 in the presence of Cu^{2+} is ca. 60 mV at pH = 8, whereas for L^4 the maximum electrochemical shift was ca. 100 mV for Cu^{2+} at the same pH.[14] In conclusion, L^1 and L^2 are redox-active functionalised molecules that can electrochemically sense Pb^{2+} (L^1) and Cu^{2+}, Zn^{2+}, and Cd^{2+} (L^2) using electrochemical methods.

Fluorescence Behaviour

The study of the fluorescence behaviour of the L^1 and L^2 ligands was also carried out in dioxane/water (70:30) mixtures and with modulation of the pH. The ligands L^1 and L^2 show typical structured anthracene-like absorption and emission spectra with a maximum in the absorption band at 366 nm for L^1 and 367 nm for L^2, and with maximum emission wavelengths at 412 and 414 nm, respectively (see photophysical data in Table 4). The fluorescence intensity of L^1 and L^2 shows the typical behaviour of anthrylmethyl-substituted polyamines with maximum fluorescence at acidic pH and decrease of fluorescence at basic pH (see Figure 3 for the fluorescence emission titration curves of L^1 and L^2). This pH-dependent emission behaviour is well

Table 4. Photophysical parameters

	λ_{exc}	λ_{emi}	φ[a]
L^1	366	412	0.0030
L^5	366	410	0.0080
L^6	366	411	0.0055

[a] Quantum yield relative to anthracene in acetonitrile (φ = 0.36).

known and attributed to the existence of electron-transfer paths from the lone pair of the amine to the photo-excited state of the anthracene at basic pH that is not operative upon amine protonation.[16] From Figure 3 it can be observed that the fully protonated species of H_2L^1 are fluorescent, whereas deprotonation of at least one nitrogen atom gave species showing a much weaker emission intensity. In line with this behaviour, the species L^2 and L^2H^+ display low fluorescence; $L^2H_2^{2+}$ and $L^2H_3^{3+}$ induce some fluorescence enhancement, but the emission enhancement is at a maximum with the fully protonated $L^2H_4^{4+}$ species.

Figures 4 and 5 show the fluorescent emission titration curves for L^1 and L^2 in the presence of Cu^{2+} and Pb^{2+} (1:1 metal/ligand ratio). In both cases, Cu^{2+} is the only metal ion able to produce a considerable modification of the emission intensity versus pH profile of the free ligand. In contrast, Pb^{2+} [shown in Figure 4 (bottom) and Figure 5 (bottom)] and the cations Ni^{2+}, Zn^{2+}, Cd^{2+}, and Hg^{2+} (not shown) do not change significantly the fluorescence emission versus pH curves of the free receptors. Figure 4 (top) shows that all four complexes $[Cu(HL^1)]^{3+}$, $[Cu(L^1)]^{2+}$, $[Cu(L^1)(OH)]^+$, and $[Cu(L^1)(OH)_2]$ induce enhancement of the emission fluorescence intensity. The quantum yield of L^1 at pH = 7 is 0.050, whereas in the presence of Cu^{2+} the quantum yield at the same pH is 0.10. Figure 5 (top) also shows that all the Cu^{2+} complexes induce fluorescence emission enhancement.

The fluorescence curve in the presence of Pb^{2+} is very close to that found for the free receptors. At this point it has to be noted that a similar effect has been observed for instance in zinc(II) complexes of *N*,*N*-dibenzylated- or *N*-(anthrylmethyl)polyazaalkanes; that is, despite the formation of stable complexes the fluorescence behaviour versus pH of the free ligand and in the presence of Zn^{2+} is very similar.[17] From Figure 4 (bottom) and Figure 5 (bottom) it can be deduced that, except for the $[Pb(HL)]^{3+}$ complex (L = L^1 or L^2), that slightly enhances the fluorescence, the remaining species, $[Pb(L)]^{2+}$, $[Pb(L)(OH)]^+$, and $[Pb(L)(OH)_2]$, do not increase the emission intensity of the free L^1 receptor. This indicates that the coordination of Pb^{2+} to the nitrogen atoms is less effective than protonation in preventing photo-induced electron-transfer processes, and that the Pb^{2+} cation has little effect on the fluorescence behaviour despite the formation of stable complexes. One possible explanation of this observed behaviour could be related to the strength of the coordination between the nitrogen atoms and the Pb^{2+} cation, a poor coordination with at least one nitrogen atom will not hinder the photo-electron transfer from the lone pair of the nitrogen atom to the excited fluorophore. In this sense the effect is similar to that observed with protons; only when the L^1 or L^2 molecules are fully protonated there is an emission enhancement, whereas partial protonations have a lesser effect or no effect at all.

The fluorescent response of L^1 and L^2 in the presence of Cu^{2+} is remarkably different to the response observed for Cu^{2+} for similar receptors. The usual behaviour observed with anthrylaza macrocycles in the presence of Cu^{2+} is a fluorescence quenching upon complexation.[18] The chelation-enhanced quenching (CHEQ) has been reported to occur with copper and also with other open-shell paramagnetic or easily reducible metal cations. In fact, for the receptor 1,4,8,11-tetrakis(naphthylmethyl)-1,4,8,11-tetraazacyclotetradecane (containing four naphthylmethyl groups attached to the four N-donor atoms of the cyclam unit) the presence of Cu^{2+} (and also Hg^{2+}) produces a noticeable quenching of the emission fluorescent intensity at acidic pH.[19] A similar effect, the quenching of the emission fluorescence, is observed for cyclam functionalised with $Ru(tpy)_2^{2+}$ groups in the presence of Cu^{2+}.[20] All these reported data contrast with the fluorescence enhancement observed for L^1 and L^2 upon complexation of Cu^{2+}. This result could be of interest because in sensing processes fluorescence enhancement rather than quenching is usually preferred in order to observe a high signal output. However, it has to be pointed out that there are a few papers reporting enhancement of the fluorescence upon copper(II) complexation.[21] This has been achieved for instance by controlling either the interaction of the metal ion with the receptor in order to reduce the metal−fluorophore interaction or acting directly modifying the nature of the fluorophore. Thus, Bharadwaj has reported that the use of preorganised cryptands can induce unusual geometries that suppress the redox activity of the coordinated Cu^{II} cation, inhibiting the interaction between the copper(II) and the photo-excited state of anthryl fluorescent groups.[21a] In a recent paper Samanta reports the development of a receptor that suffers enhancement upon addition of metal ions by simply using electron-deficient fluorophores.[21b]

In our case we believe that the anomalous behaviour observed for Cu^{2+} could be ascribed to the presence of the ferrocenyl groups (see below). It is well known that ferrocene is an efficient fluorescence quencher via both energy-transfer and reductive quenching processes.[10d] In our case, the occurrence of an electron-transfer mechanism is thermodynamically favourable as it can be demonstrated from electrochemical and photophysical data. The free energy of the process (anthracene + Fc = anthracene$^-$ + Fc$^+$) in which the ferrocene is acting as reductive quencher can be calculated by the equation of Rehm-Weller, where $E^0_{Fc^+/Fc}$ and E^0_{fl/fl^-} are the redox potentials of the processes $Fc^+ + 1e^- \rightarrow Fc$ and $fl + 1e^- \rightarrow fl^-$ (fl = fluorophore), respectively, and λ can be obtained from the emission fluorescence spectrum.[22]

$$\Delta G = -\frac{hcN_A}{\lambda} + F\left[E^o_{Fc^+/Fc} - E^o_{fl/fl^-}\right]$$

Redox potentials were measured in dry acetonitrile (0.1 M tetrabutylammonium perchlorate; 25 °C). The ligand L^2 shows a reversible oxidation process at 450 mV and a reduction irreversible wave at −2.2 V versus SCE, which have been ascribed to the oxidation of the ferrocenyl and to the reduction of the anthryl groups, respectively. Taking into account these data, ΔG is −33.6 kJ/mol indicating that photo-induced electron transfer from the ferrocene to the anthryl fluorophore can occur. Additionally, an energy-

transfer quenching mechanism could also be possible.[10d] The quenching induced by the ferrocenyl group is supported by experimental data, thus the quantum yield of the ferrocene-containing ligand L^1 in acetonitrile ($\varphi = 0.0030$) is lower than that of L^6 ($\varphi = 0.0055$) or L^5 ($\varphi = 0.0080$). This difference in quantum yield is ascribed to the presence of ferrocenylmethyl groups in L^1. In fact, when stoichiometric amounts of H_2O_2 were added to L^1, the solution turned green-blue (due to the oxidation of ferrocene) and there was a fluorescence enhancement (quantum yield of ca. 0.0042).

As stated above, Cu^{2+} is also a well-known quencher. From a thermodynamic point of view both energy-transfer or electron-transfer processes are possible when Cu^{2+} ions are added to L^1 or L^2 solutions. Bearing this in mind, one would expect that the presence of Cu^{2+} would reduce even more the emission intensity of the receptors. In contrast, an enhancement of the fluorescence is observed. However, it has to be taken into account that, although the presence of Cu^{2+} gives new quenching routes, it might also inhibit some. Namely, strong coordination to nitrogen atoms can inhibit the photo-electron transfer from the lone pair of the amine to the fluorophore. Additionally, it might also happen that the presence of Cu^{2+} hinders the energy-transfer quenching process from the ferrocene to the anthracene due to the increase of the rigidity of the receptor upon coordination, thereby disfavouring the nonradiative decay processes. Furthermore, and especially for L^2, the cation Cu^{2+} induces a significant cathodic electrochemical shift of the ferrocenyl redox potential of ca. 60 mV in dioxane/water and of ca. 100 mV in acetonitrile making electron transfer from the ferrocene to the anthracene thermodynamically less favourable. In resume, although Cu^{2+} itself might introduce energy- and electron-transfer quenching paths it also inhibits other quenching mechanisms, the overall effect being an emission fluorescence enhancement.

Anion Sensing

The free receptors L^1 and L^2 are anion-insensitive. Thus, addition of different anions such as phosphate, sulfate, nitrate, fluoride, chloride, bromide, etc. to solutions of these receptors in acetonitrile or dioxane/water resulted in no variation of either electrochemical or photochemical properties. This contrasts with the anion-sensing ability found for the $[Cu(L^2)]^{2+}$complex (see below). In this sense it is noticeable that one of the most interesting features in the crystallographic characterisation of the $[Cu(L^2)]^{2+}$ complex is the formation of a host molecule containing a Cu^{2+} ion surrounded by a cavity built with three ferrocenylmethyl and one anthrylmethyl group. This is a peculiar topology. The interaction (either covalent or electrostatic) of anions with the Cu^{2+} charged cation might allow a close proximity between the guest (anion) and the electro-active ferrocenyl or the photo-active anthryl signalling units. In order to check this possible co-operative effect, the anion-sensing properties of the $[Cu(L^2)]^{2+}$complex was investigated electrochemically and by fluorescence studies. Table 5 summarises the electrochemical data in acetonitrile. The most remarkable effect is the very large cathodic shift of 210 mV observed upon fluoride addition. Other halide anions such as chloride and bromide gave much lower cathodic shifts (ca. 20 mV). Thus, the $[Cu(L^2)]^{2+}$complex is able to selectively and electrochemically sense fluoride over other halide anions.[23] The $H_2PO_4^-$ anion also induces an important electrochemical cathodic shift of 150 mV whereas the response in the presence of HSO_4^-, and NO_3^- is remarkably lower.[24] Fluorescence studies on the $[Cu(L^2)]^{2+}$complex upon addition of anions in acetonitrile were also carried out. Table 5 summarises the anion response. The addition of Cl^-, Br^-, I^-, and HSO_4^- had no effect, whereas nitrate, fluoride and $H_2PO_4^-$ induced an enhancement of the fluorescence intensity of the $[Cu(L^2)]^{2+}$ complex of 26%, 20%, and 17%, respectively. From fluorimetric/spectroscopic titration well-defined isosbestic points were observed indicating the formation of 1:1 complexes. The logarithms of the stability constants obtained by least-squares analysis of the titration curves were 4.5 ± 0.2; 4.2 ± 0.1, and 4.4 ± 0.3 for nitrate, fluoride, and dihydrogenophosphate, respectively.[25]

Table 5. Photophysical and electrochemical anion response of $[Cu(L^2)]^{2+}$ upon addition of 10 equiv. of the corresponding anion in acetonitrile

Electrochemical							
Receptor	$H_2PO_4^-$	HSO_4^-	NO_3^-	F^-	Cl^-	Br^-	
$[Cu(L^2)]^{2+}$	150[a]	55	< 5	210	24	20	
Photophysical							
Receptor	$H_2PO_4^-$	HSO_4^-	NO_3^-	F^-	Cl^-	Br^-	I^-
$[Cu(L^2)]^{2+}$	17%[b]	< 5%	26%	20%	< 5%	< 5%	< 5%

[a] ΔE_{pa} calculated as E_{pa} of the receptor $-E_{pa}$ of the receptor anion in mV for $[Cu(L^2)]^{2+}$ in 0.1 M tetrabutylammonium perchlorate. Iodide has an oxidation potential in acetonitrile similar to that of ferrocene and was not studied. [b] Enhancement of the fluorescence intensity of the 412-nm emission band.

Conclusions

We can conclude that L^1 and L^2 are rare receptors, containing two signalling subunits whose response against metal cations can be controlled by the type of output signal (electrochemical shift or changes in fluorescence emission) used to trace information from the solution. This is resumed in Table 6 that shows the selective response obtained by the oxaaza ring 1,4,10-trioxa-7,13-diazacyclopentadecane or the polyaza ring 1,4,8,11-tetraazacyclotetradecane depending on their functionalisation. Difunctionalised systems could have advantages over monofunctionalised ones because the former might act as multiple-sensing receptors. Thus, L^1 responds to Pb^{2+} using electrochemical methods, but is a Cu^{2+} chemosensor if emission intensity is used as output signal. In a similar way, L^2 electrochemically responds to Cu^{2+}, Zn^{2+}, and Cd^{2+} but it only gives emission response against Cu^{2+}. A similar control effect on the sens-

Table 6. Electrochemical and photophysical response against certain transition metal ions by the functionalised binding domains 1,4,10-trioxa-7,13-diazacyclopentadecane and 1,4,8,11-tetraazacyclotetradecane functionalised with ferrocene and anthracene

	Ferrocene	Anthracene	Ferrocene and Anthracene
1,4,10-Trioxa-7,13-diazacyclopentadecane	Pb^{2+}, Cd^{2+}, Hg^{2+}	Hg^{2+}	Electrochemical: Pb^{2+} Photophysical: Cu^{2+}
1,4,8,11-Tetraazacyclotetradecane	Cu^{2+}, Zn^{2+}, Cd^{2+}	–	Electrochemical: Cu^{2+}, Zn^{2+}, Cd^{2+} Photophysical: Cu^{2+}

ing process depending on the output signal, is observed for the $[Cu(L^2)]^{2+}$complex in its interaction with anions. Thus, the maximum electrochemical shift is observed in the presence of fluoride, whereas the largest emission fluorescence enhancement was observed upon addition of the poorly coordinating anion nitrate.

Experimental Section

General Remarks: All commercially available reagents were used without further purification. Air/water-sensitive reactions were performed in flame-dried glassware under argon. Dioxane and acetonitrile were dried with CaH_2 and distilled prior to use.

L^1: The free base 1,4,10-trioxa-7,13-diazacyclopentadecane (400 mg, 1.832 mmol) was heated under reflux in dry dichloromethane with 9-(chloromethyl)anthracene (410 mg, 1.805 mmol) in the presence of triethylamine (560 mg, 5.5 mmol). After 6 h, the mixture was cooled to room temperature, basic water was added and the organic phase separated, dried with anhydrous magnesium sulfate, filtered, and concentrated to dryness. The resulting oil was dissolved in dichloromethane and purified by chromatography on alumina using dichloromethane/ethanol (100:1, v/v) as eluent. This allowed us to isolate the compound 7-anthracenylmethyl-1,4,10-trioxa-7,13-diazacyclopentadecane. Yield 450 mg, 56%. This compound (415 mg, 1.015 mmol) was heated under reflux in dry acetonitrile with (ferrocenylmethyl)trimethylammonium iodide (508 mg, 1.32 mmol) in the presence of potassium carbonate. After 24 h, the reaction mixture was filtered and the orange solution concentrated to dryness. The product L^1 was obtained after chromatography on alumina using dichloromethane/ethanol (100:1, v/v) as eluent. Yield 615 mg, 67%. ^{1}H NMR ($CDCl_3$): δ = 2.65 (dt, 4 H, CH_2), 2.81 (t, 2 H, CH_2), 2.96 (t, 2 H, NCH_2), 3.55 (m, 14 H, CH_2), 4.09 (t, 2 H, C_5H_4), 4.10 (s, 5 H, C_5H_5), 4.14 (t, 2 H, C_5H_4), 4.55 (s, 2 H, CH_2), 7.48 (m, 4 H, CH_{anthr}), 8.00 (d, 2 H, CH), 8.40 (s, 1 H, CH), 8.55 (d, 2 H, CH_{anthr}). ^{13}C {^{1}H} NMR ($CDCl_3$): δ = 52.1, 53.2, 53.5, 53.6, 54.2, 55.5 (CH_2), 67.9, 68.4, 69.1 (CH, Cp), 70.1, 70.3, 70.4 (CH_2O), 124.7, 125.2, 125.5, 127.3, 128.8, 130.3, 131.3, 131.3 (CH_{anthr}). MS (FAB): *m*/*z* = 607 [M^+]. $C_{36}H_{42}FeN_2O_3{\cdot}3H_2O$ (660): calcd. C 65.5, H 6.4, N 4.3; found C 65.5, H 6.3, N 4.2.

L^2: The polyazacycloalkane 1,4,8,11-tetraazacyclotetradecane (520 mg, 2.6 mmol) was heated under reflux in absolute ethanol with 9-(chloromethyl)anthracene (560 mg, 2.6 mmol) in the presence of triethylamine. After 16 h, the mixture was cooled to room temperature and the solvent was removed. To the residue basic water and dichloromethane were added and the organic phase was separated, dried with anhydrous magnesium sulfate, filtered, and concentrated to dryness. The resulting oil was dissolved in dichloromethane and purified by chromatography on alumina using dichloromethane/ethanol (100:3, v/v) as eluent. This allowed us to isolate the compound 1-anthrylmethyl-1,4,8,11-tetraazacyclotetradecane. Yield 280 mg, 28%. This compound (280 mg, 0.717 mmol) was heated under reflux in dry acetonitrile with (ferrocenylmethyl)trimethylammonium iodide (1103 mg, 2.868 mmol) in the presence of potassium carbonate. After 24 h, the reaction mixture was filtered and the orange solution concentrated to dryness. The product L^2 was obtained after column chromatography on alumina using dichloromethane/ethanol (100:1, v/v) as eluent. Yield 565 mg, 80%. ^{1}H NMR ($CDCl_3$): δ = 1.55 (q, 2 H, $CH_2CH_2CH_2$), 1.75 (q, 2 H, $CH_2CH_2CH_2$), 2.00 (t, 4 H, N$CH_2CH_2CH_2$N), 2.28−2.70 (m, 12 H, NCH_2CH_2N), 3.36, 3.28, 3.15 (s, 6 H, CH_2), 3.84 (t, 2 H, C_5H_4), 3.90 (t, 2 H, C_5H_4), 3.93 (s, 5 H, C_5H_5), 3.99 (t, 2 H, C_5H_4), 4.01 (s, 5 H, C_5H_5), 4.02 (t, 4 H, C_5H_4), 4.05 (s, 5 H, C_5H_5), 4.07 (t, 2 H, C_5H_4), 4.31 (s, 2 H, CH_2), 7.48 (m, 4 H, CH_{anthr}), 8.00 (d, 2 H, CH), 8.40 (s, 1 H, CH), 8.55 (d, 2 H, CH_{anthr}).^{13}C {^{1}H} NMR ($CDCl_3$): δ = 24.1, 24.8 ($CH_2CH_2CH_2$), 47.0, 49.0, 49.6, 49.7, 50.3, 50.4, 51.0, 51.3, 51.4, 53.3, 53.4, 54.1 (CH_2N), 67.6, 67.7, 68.2, 68.3, 68.4, 70.1, 70.2, 70.3 (CH, Cp), 124.8, 125.1, 126.1, 127.0, 128.7, 131.2, 131.4, 131.5 (CH_{anthr}). MS (FAB): 985 [M^+]. $C_{56}H_{64}Fe_3N_4{\cdot}3H_2O$ (1014): calcd. C 67.0, H 6.6, N 5.2; found C 67.1, H 6.7, N 5.4.

Structure Determination of $[H_2L^1][PF_6]_2{\cdot}0.5CH_2Cl_2{\cdot}H_2O$: $C_{36.5}H_{44}ClF_{12}FeN_2O_4P_2$, M = 955.98, triclinic, space group $P\bar{1}$, a = 12.176(2), b = 12.787(2), c = 15.589(2) Å, α = 95.716(11), β = 110.088(12), γ = 106.236(12) °, Z = 2, V = 2136.1(5) Å^3, $D_{calcd.}$ = 1.486 g cm^{-3}, λ(Mo-K_α) = 0.71069 Å, T = 293(2) K, μ(Mo-K_α) = 0.583 mm^{-1}. Measurements were carried out using a Siemens P4 diffractometer with graphite-monochromated Mo-K_α radiation on a yellow crystal of dimensions 0.10 × 0.20 × 0.27 mm. A total of 5844 reflections was collected of which 5532 were independent (R_{int} = 0.0143). Lorentz, polarisation and absorption (ψ-scan, max. and min. transmission 0.541 and 0.014) corrections were applied. The structure was solved by direct methods (SHELXTL)[26] and refined by full-matrix least-squares analysis on F^2 (SHELXTL). The refinement converged at $R1$ = 0.084 [$F > 4\sigma(F)$] and $wR2$ = 0.249 (all data). Largest peak and hole in the final difference map +0.75 and −0.41 e Å^{-3}.

Structure Determination of $[CuL^2][PF_6]_2{\cdot}CH_2Cl_2$: $C_{59}H_{66}Cl_2CuF_{12}Fe_3N_4P_2$, M = 1423.09, monoclinic, space group $P2_1/c$, a = 14.419(5), b = 35.644(9), c = 13.282(4) Å, β = 104.20(3) °, Z = 4, V = 6618(3) Å^3, $D_{calcd.}$ = 1.428 g cm^{-3}, λ(Mo-K_α) = 0.71069 Å, T = 293(2) K, μ(Mo-K_α) = 1.163 mm^{-1}. Measurements were carried out using a Siemens P4 diffractometer with graphite-monochromated Mo-K_α radiation on a yellow crystal of dimensions 0.15 × 0.15 × 0.23 mm. A total of 9086 reflections was collected of which 8645 were independent (R_{int} = 0.0985). Lorentz, polarisation and absorption (ψ-scan, max. and min. transmission 0.3133 and 0.2912) corrections were applied. The structure was solved by direct methods (SHELXTL) [26] and refined by full-matrix least-squares analysis on F^2 (SHELXTL). The refinement converged at $R1$ = 0.1008 [$F > 4\sigma(F)$] and $wR2$ = 0.3609 (all data). Largest peak and hole in the final difference map +0.78 and −0.63 e Å^{-3}.

Crystallographic data for the structures reported in this paper have been deposited with the Cambridge Crystallographic Data Centre as supplementary publication no. CCDC-158668 ($[H_2L^1][PF_6]_2 \cdot 0.5CH_2Cl_2 \cdot H_2O$) and -158669 ($[CuL^2][PF_6]_2 \cdot CH_2Cl_2$). Copies of the data can be obtained free of charge on application to CCDC, 12 Union Road, Cambridge CB2 1EZ, UK [Fax: (internat.) + 44-1223/336-033; E-mail: deposit@ccdc.cam.ac.uk].

Physical Measurements: The fluorescence behaviour was studied with a FS900CDT Steady State T-Geometry Fluorimeter, Edinburgh Analytical Instruments. All solutions for photophysical studies were previously degassed. The concentration of ligands and metal ions were ca. 1.0×10^{-4} M in dioxane/water (the metal ions were perchlorate or nitrate salts of Ni^{2+}, Cu^{2+}, Zn^{2+}, Cd^{2+}, Hg^{2+}, and Pb^{2+}). The fluorescence quantum yield of anthracene [27] in acetonitrile was used as standard and taken to be 0.36. In order to obtain the quantum yield of the new ligands, those were dissolved in acetonitrile, their absorbance adjusted to ca. 0.15 and then compared to the standard. The ^1H NMR spectra were recorded with a Varian Gemini spectrometer. Chemical shifts are reported in ppm downfield from the TMS signal. Spectra taken in $CDCl_3$ were referenced to residual $CHCl_3$. Potentiometric titrations were carried out in 1,4-dioxane/water (70:30, v/v; 0.1 M KNO_3) using a reaction vessel that was thermostatically controlled using water at 25.0 ± 0.1 °C under nitrogen. The titrant was added by a Crison microburete 2031. The potentiometric measurements were made using a Crison 2002 pH-meter and a combined glass electrode. The titration system was automatically controlled using a PC. The electrode was calibrated as a hydrogen concentration prove by titration of well-known amounts of HCl with CO_2-free KOH solution and determining the equivalent point by the Gran's method which gives the standard potential E'° and the ionic product of water ($K'_w = [H^+][OH^-]$). The concentration of the metal ions was determined using standard methods. The computer program SUPERQUAD [28] was used to calculate the protonation and stability constants. The titration curves for each system (ca. 250 experimental points corresponding to at least three titration curves, pH = −log [H] range investigated 2.2−10.3, concentration of the ligand and metal ion being ca. 1.2×10^{-3} M) were treated either as a single set or as separated entities without significant variations in the values of the stability constant. Finally, the data sets were merged and treated simultaneously to give the stability constant. Electrochemical data were carried out in 1,4-dioxane/water (70:30, v/v) and in dry acetonitrile, with a programmable function generator Tacussel IMT-1, connected to a Tacussel PJT 120−1 potentiostat. The concentration of ligands and metal ions were ca. 1.0×10^{-3} M in dioxane/water (the metal ions were perchlorate or nitrate salts of Cu^{2+} and Pb^{2+}; metal-to-ligand ratio 1:1). The working electrode was platinum with a saturated calomel reference electrode separated from the test solution by a salt bridge containing the solvent/supporting electrolyte. The auxiliary electrode was platinum wire. $E_{1/2}$ values were measured by rotating-disc electrode experiments (scan speed 10 mVs^{-1}, rotating speed 7000 revolutions min^{-1}).

Acknowledgments

We thank the DGICYT (proyectos PB98−1430-C02−02, 1FD97−0508-C03−01 and AMB99−0504-C02−01) for support. F. S. also thanks the Ministerio de Ciencia y Tecnología for a Doctoral Fellowship.

[1] [1a] J.-M. Lehn, *Supramolecular Chemistry: Concept and Perspective*, VCH Verlagsgesellschaft, **1996**, Weinheim. [1b] E. C. Constable, *Comprehensive Supramolecular Chemistry* (Ed: J.-M. Lehn), Pergamon, Oxford, **1996**, vol. 9.

[2] [2a] M. Takagi, K. Ueno, *Top. Curr. Chem.* **1984**, *121*, 39−65. [2b] H. G. Löhr, F. Vögtle, *Acc. Chem. Res.* **1985**, *18*, 65−72.

[3] See for example: [3a] F. C. J. M. van Veggel, W. Verboom, D. N. Reinhoudt, *Chem. Rev.* **1994**, *94*, 279−299. [3b] R. Martínez-Mañez, J. Soto, J. M. Lloris, T. Pardo, *Trends Inorg. Chem.* **1998**, *5*, 183−203. [3c] P. D. Beer, *Acc. Chem. Res.* **1998**, *31*, 71−80.

[4] See for example: [4a] A. P. de Silva, H. Q. N. Gunaratne, T. Gunnlaugsson, A. J. M. Huxley, C. P. McCoy, J. T. Rademacher, T. E. Rice, *Chem. Rev.* **1997**, *97*, 1515−1566. [4b] A. W. Czarnik, *Acc. Chem. Res.* **1994**, *27*, 302−308. [4c] Special Issue on Luminescent Sensors of *Coord. Chem. Rev.* **2000**, *205*, 1−232.

[5] See for example: [5a] O. Brümmer, J. J. La Clair, K. D. Janda, *Org. Lett.* **1999**, *1*, 415−418. [5b] H. Miyaji, J. L. Sessler, *Angew. Chem. Int. Ed.* **2001**, *40*, 154−157. [5c] H. Miyaji, W. Sato, J. L. Sessler, *Angew. Chem. Int. Ed.* **2000**, *39*, 1777−1780. [5d] F. Sancenón, A. B. Descalzo, R. Martínez-Máñez, M. A. Miranda, J. Soto, *Angew. Chem. Int. Ed.* **2001**, *40*, 2640−2643.

[6] See for example: [6a] P. D. Beer, J. Cadman, J. M. Lloris, R. Martínez-Máñez, J. Soto, T. Pardo, M. D. Marcos, *J. Chem. Soc., Dalton Trans.* **2000**, 1805−1812. [6b] J. M. Lloris, R. Martínez−Máñez, T. Pardo, J. Soto, M. E. Padilla-Tosta, *Chem. Commun.* **1998**, 837−838. [6c] H. Plenio, C. Aberle, Y. Al Shihadeh, J. M. Lloris, R. Martínez-Máñez, T. Pardo, J. Soto, *Chem. Eur. J.* **2001**, *7*, 2848−2861.

[7] See for example: [7a] H. F. Ji, R. Dabestani, G. M. Brown, *J. Am. Chem. Soc.* **2000**, *122*, 9306−9307. [7b] K. Rurack, W. Rettig, U. Resch-Geuger, *Chem. Commun.* **2000**, 407−408. [7c] T. Hirano, K. Kikuchi, Y. Urano, T. Higuchi, T. Nagano, *Angew. Chem. Int. Ed.* **2000**, *39*, 1052−1054. [7d] E. Kimura, T. Koike, *Chem. Soc. Rev.* **1998**, *27*, 179−184. [7e] L. Fabbrizzi, M. Licchelli, P. Pallavicini, L. Prodi, *Angew. Chem. Int. Ed.* **1998**, *37*, 800−802.

[8] See for example: [8a] B. L. Feringa, W. F. Jager, B. De Lange, *Tetrahedron* **1993**, *49*, 8267−8310. [8b] D. R. Walt, *Acc. Chem. Res.* **1998**, *31*, 267−278. [8c] M. Ahmad, H. Hamzah, E. S. Marsoun, *Talanta* **1998**, *47*, 275−283.

[9] See for example: [9a] A. Doron, E. Katz, M. Portnoy, I. Willner, *Angew. Chem. Int. Ed. Engl.* **1996**, *35*, 1535−1537. [9b] G. Zotti, G. Schiavon, S. Zecchin, *Langmuir* **1998**, *14*, 1728−1733. [9c] G. Zotti, G. Schiavon, S. Zecchin, A. Berlin, G. Pagani, A. Canavesi, *Langmuir* **1997**, *13*, 2694−2698.

[10] [10a] P. D. Harvey, L. Gan, C. Aubry, *Can. J. Chem.* **1990**, *68*, 2278−2288. [10b] P. D. Harvey, L. Gan, *Inorg. Chem.* **1991**, *30*, 3239−3241. [10c] B. Delavaux-Nicot, S. Fery-Forgues, *Eur. J. Inorg. Chem.* **1999**, 1821−1825. [10d] P. D. Beer, F. Szemes, V. Balzani, C. M. Salà, M. G. B. Drew, S. W. Dent, M. Maestri, *J. Am. Chem. Soc.* **1997**, *119*, 11864−11875. [10e] U. Siemeling, U. Vorfeld, B. Neumann, H. G. Stammler, P. Zanello, F. F. De Biani, *Eur. J. Inorg. Chem.* **1999**, 1−5.

[11] L. F. Lindoy, *The Chemistry of Macrocyclic Ligand Complexes*, Cambridge University Press, Cambridge, **1989**.

[12] M. J. L. Tendero, A. Benito, J. Cano, J. M. Lloris, R. Martínez-Máñez, J. Soto, A. J. Edwards, P. R. Raithby, M. A. Rennie, *J. Chem. Soc., Chem. Commun.* **1995**, 1643−1644.

[13] J. M. Lloris, R. Martínez-Máñez, M. E. Padilla-Tosta, T. Pardo, J. Soto, P. D. Beer, J. Cadman, D. K. Smith, *J. Chem. Soc., Dalton Trans.* **1999**, 2359−2369.

[14] J. M. Lloris, R. Martínez-Máñez, T. Pardo, J. Soto, M. E. Padilla−Tosta, *J. Chem. Soc., Dalton Trans.* **1998**, 2635−2641.

[15] [15a] A. Benito, R. Martínez-Máñez, J. Payá, J. Soto, M. J. L. Tendero, E. Sinn, *J. Organomet. Chem.* **1995**, *503*, 259−263. [15b] M. J. L. Tendero, A. Benito, R. Martínez-Máñez, J. Payá, A. J. Edwards, P. R. Raithby, *J. Chem. Soc., Dalton Trans.* **1996**, 343−351.

[16] [16a] A. P. de Silva, T. Gunnlaugsson, T. E. Rice, *Analyst* **1996**, *121*, 1759−1762. [16b] L. Fabbrizzi, M. Licchelli, P. Pallavicini, D. Sacchi, A. Taglietti, *Analyst* **1996**, *121*, 1763−1768.

[17] [17a] F. Pina, M. A. Bernardo, E. García-España, *Eur. J. Inorg. Chem.* **2000**, 2143−2157. [17b] S. Alves, F. Pina, M. T. Albelda, E. García-España, C. Soriano, S. V. Luis, *Eur. J. Inorg. Chem.* **2001**, 405−412.

[18] [18a] L. Fabbrizzi, M. Licchelli, P. Pallavicini, A. Perotti, D. Sacchi, *Angew. Chem. Int. Ed. Engl.* **1994**, *33*, 1975−1977. [18b] G. De Santis, L. Fabbrizzi, M. Licchelli, C. Mangano, D. Sacchi, N. Sardone, *Inorg. Chim. Acta.* **1997**, 69−76. [18c] J. Yoon, N. E. Ohler, D. H. Vance, W. D. Aumiller, A. W. Czarnik, *Tetrahedron Lett.* **1997**, *38*, 3845−3848. [18d] L. Fabbrizzi, M. Licchelli, L. Parodi, A. Poggi, A. Taglietti, *Eur. J. Inorg. Chem.* **1999**, 35−39.

[19] Y. Al Shihadeh, A. Benito, J. M. Lloris, R. Martínez-Máñez, T. Pardo, J. Soto, M. D. Marcos, *J. Chem. Soc., Dalton Trans.* **2000**, 1199−1205.

[20] M. E. Padilla-Tosta, J. M. Lloris, R. Martínez-Máñez, A. Benito, J. Soto, T. Pardo, M. A. Miranda, M. D. Marcos, *Eur. J. Inorg. Chem.* **2000**, 741−748.

[21] [21a] P. Ghosh, P. Bharadwaj, S. Mandal, S. Ghosh, *J. Am. Chem. Soc.* **1996**, *118*, 1553−1554. [21b] B. Ramachandram, A. Samanta, *Chem. Commun.* **1997**, 1037−1038. [21c] M. Narita, Y. Higuchi, F. Hamada, H. Kumagai, *Tetrahedron Lett.* **1998**, *39*, 8687−8690. [21d] K. Kubo, T. Sakurai, A. Mori, *Talanta* **1999**, *50*, 73−77. [21e] K. Rurack, M. Kollmannsberger, U. Resch-Genger, J. Daub, *J. Am. Chem. Soc.* **2000**, *122*, 968−969.

[22] D. Rehm, A. Weller, *Isr. J. Chem.* **1970**, *8*, 259.

[23] See for example: [23a] M. Staffilani, K. S. B. Hancock, J. W. Steed, K. T. Holman, J. L. Atwood, R. K. Junega, R. S. Burkhalter, *J. Am. Chem. Soc.* **1997**, *119*, 6324−6335. [23b] C. Dusemund, K. R. A. S. Sandanayake, S. Shinkai, *J. Chem. Soc., Chem. Commun.* **1995**, 333−334.

[24] See for example: [24a] P. D. Beer, M. G. B. Drew, A. R. Graydon, D. K. Smith, S. E. Stokes, *J. Chem. Soc., Dalton Trans.* **1995**, 403−408. [24b] P. D. Beer, J. Cadman, J. M. Lloris, R. Martínez-Máñez, J. Soto, T. Pardo, M. D. Marcos, *J. Chem. Soc., Dalton Trans.* **2000**, 1805−1812. [24c] P. D. Beer, J. Cadman, J. M. Lloris, R. Martínez-Máñez, M. E. Padilla, T. Pardo, D. K. Smith, J. Soto, *J. Chem. Soc., Dalton Trans.* **1999**, 127−133. [24d] C. Valério, J.-L. Fillaut, J. Ruíz, J. Guittard, J.-C. Blais, D. Astruc, *J. Am. Chem. Soc.* **1997**, *119*, 2588−2589.

[25] J. Bourson, J. Pouget, B. Valeur, *J. Phys. Chem.* **1993**, *97*, 4552−4557.

[26] SHELXTL, Version 5.03, Siemens Analytical X-ray Instruments, Madison, WI, **1994**.

[27] I. B. Berlman, *Handbook of Fluorescence Spectra of Aromatic Molecules*, Academic Press, New York, **1971**.

[28] P. Gans, A. Sabatini, A. Vacca, *J. Chem. Soc., Dalton Trans.* **1995**, 1195−1200.

Received July 13, 2001
[I01271]